

# Finite-size scaling for four-dimensional Higgs-Yukawa model near the Gaussian fixed point

David Y.-J Chu<sup>a</sup>, Karl Jansen<sup>b</sup>, Bastian Knippschild<sup>c</sup>, C.-J. David Lin<sup>d,e</sup>

<sup>a</sup> Department of Electrophysics, National Chiao-Tung University, Hsinchu 30010, Taiwan

<sup>b</sup> NIC, DESY Zeuthen, D-15738 Zeuthen, Germany

<sup>c</sup> HISKP, Universität Bonn, D-53115 Bonn, Germany

<sup>d</sup> Institute of Physics, National Chiao-Tung University, Hsinchu 30010, Taiwan

<sup>e</sup> Centre for High Energy Physics, Chung-Yuan Christian University, Chung-Li 32023, Taiwan

## Abstract:

We analyse finite-size scaling behaviour of a four-dimensional Higgs-Yukawa model near the Gaussian infrared fixed point. Through improving the mean-field scaling laws by solving one-loop renormalisation group equations, the triviality property of this model can be manifested in the volume-dependence of moments of the scalar-field zero mode. The scaling formulae for the moments are derived in this work with the inclusion of the leading-logarithmic corrections. To test these formulae, we confront them with data from lattice simulations in a simpler model, namely the  $O(4)$  pure scalar theory, and find numerical evidence of good agreement. Our results of the finite-size scaling can in principle be employed to establish triviality of Higgs-Yukawa models, or to search for alternative scenarios in studying their fixed-point structure, if sufficiently large lattices can be reached.

PACS numbers: 11.15.Ha, 12.38.Gc, 12.15.Ff

## I. INTRODUCTION

With the progress of experiments at the Large Hadron Collider (LHC), it is becoming essential to understand the validity of the Standard Model (SM). In particular, for the scalar sector of the SM there is very strong evidence that it is trivial [1–12], leading to the fact that the cut-off scale is indispensable, necessitating the emergence of new physics at a yet unknown energy scale. Before the discovery of the scalar resonance around 125 GeV, this triviality property was used to predict an upper bound for the Higgs-boson mass [13] which then later could indeed be computed on the lattice [14–16]. Given the experimental measurement of the Higgs-boson mass, now it can be an ingredient for the investigation of the appearance of new physics beyond the SM [17–23].

It has been a common strategy to extend the SM *via* introducing novel interactions that involve relevant operators. These relevant operators can then result in non-trivial vacuum structure, leading to dynamical electroweak symmetry breaking (dEWSB). For instance, in the walking-technicolour scenario [24–26], the SM Higgs sector is replaced by a novel gauge theory coupled to technifermions. This new gauge coupling is asymptotically free. It evolves very slowly under renormalisation group (RG) transformation, and becomes strong at the electroweak scale. In such a scenario, the technifermion condensate leads to dEWSB, and there can be a light scalar bound state because of the quasi scale invariance. In the past decade, there have been many works to search for candidate theories for such a scenario using lattice computations [27–29] and the gauge-gravity duality [30, 31]. Another example is the class of theories that are generically named the composite Nambu-Goldstone Higgs models [32–34], in which the Higgs particle is one of the Goldstone bosons in a new strongly-coupled sector beyond the SM. The Higgs boson then acquires its mass through the interaction between this new sector and the SM, which misaligns the vacuum and breaks the electroweak symmetry. In recent years, schemes for the ultraviolet (UV) completion of such models have been proposed, see, *e.g.*, Refs. [35–38]. These proposals all involve asymptotically-free gauge theories, and some of them have been studied numerically with lattice regularisation [39–44].

In the research activities described above, an important ingredient for finding physics beyond the SM is the knowledge of the fixed-point structure of candidate theories that can result in dEWSB. Amidst the significant amount of projects searching for new, relevant operators beyond the SM, we stress that our understanding for the non-perturbative aspect of the SM electroweak sector can still be improved. While it is widely accepted that the  $O(4)$  scalar theory is trivial, where no relevant operator can emerge, the situation with the Higgs-Yukawa model still requires further clarification. This is the main motivation of the current work, in which we develop a strategy for studying the fixed-point structure of the Higgs-Yukawa model by employing the technique of finite-size scaling (FSS). As pointed out in Refs. [45], perturbation theory indicates that there can be interesting phase structures in the Higgs-Yukawa model without gauge fields. In particular, a UV fixed point may be present. In such a scenario, the RG flows do not always approach the Gaussian (mean-field) fixed point in the infrared (IR) regime, and the scalar quartic operator can be relevant. This UV fixed point typically appears at the values of the couplings where perturbation theory may not be applicable [46]. Therefore it would be necessary to perform studies using nonperturbative approaches, amongst which lattice field theory is the most reliable method. Compared to the pure scalar theories, lattice investigation of the Higgs-Yukawa model is much more challenging. In particular, it is conceptually difficult to regularise chiral fermions in Lattice Field Theory. There were many lattice calculations for the phase structure and the spectrum of the Higgs-Yukawa model without the continuum-like chiral symmetry around 1990. See Refs. [47–62] for an incomplete list of them, see Ref. [63] for a proceedings article covering the attempts at that time. These early works led to evidence that the phase structures of the Higgs-Yukawa model can be very rich. In the past decade, many aspects of such studies have been extended to the case of chiral Yukawa couplings [64–70]. A thorough, detailed analysis of the scaling behaviour of the theory can provide a very useful tool to differentiate the scenarios sketched above. We emphasise that only such an analysis can lead to reliable results regarding the existence of relevant operators in the Higgs-Yukawa model.

Finite-size technique is a well established and frequently used tool for studying the scaling behaviour of a model [71]. It also combines naturally with lattice simulations. In this approach, one first looks for second-order phase transitions in the space of the bare couplings of a theory. Such phase transitions, when appearing at zero temperature and infinite volume, are the limit where the momentum cut-off approaches infinity. That is, they represent the continuum limit when the theory is regularised with the space-time lattice. In the vicinity of these transitions, the lattice size is the only available low-energy scale, and it can be regarded as the renormalisation scale. One can then use the RG equations (RGE's) to investigate the correlators and obtain their dependence on the finite size of the system. In this procedure, the presence of either a Gaussian or a non-trivial fixed point is crucial. It ensures that the dimensionless couplings approach constants, and the relevant couplings will combine with the lattice volume to result in FSS behaviour. As pointed out in Ref. [72], care has to be taken when implementing this strategy in space-time dimension

higher than three, because of issues arising from the properties of IR fixed points. It was later demonstrated [73] that for correlators in four dimensions, logarithmic corrections to the volume-dependence play an essential role in the mean-field FSS behaviour. This is actually a manifestation of the fact that logarithmic scaling is a signature of Gaussian fixed points [2]. There have been studies on these logarithms for four-dimensional scalar models [6–8]. These studies resulted in evidence that such models are indeed trivial. In the present work, we extend the FSS analysis to four-dimensional Higgs-Yukawa models, making thus a significant step beyond the existing results. In fact, to the best of our knowledge, our work is the first to derive FSS formulae for the Higgs-Yukawa models.

In this paper, we present results for our investigation of the corrections from leading logarithms (LL’s) to the mean-field scaling laws for moments of the scalar-field zero mode in a four-dimensional Higgs-Yukawa model. Our study has been performed *à la* Brezin and Zinn-Justin [73]. The main finding of this work is that the functional form of these LL-improved mean-field scaling laws can be derived, and it can be combined with lattice computations to probe the nature of fixed points in the theory. Following a scan of the bare parameter space to search for critical points by employing numerical simulations, one can then apply the strategy we develop here to confirm triviality of the Higgs-Yukawa theory, or to look for alternative scenarios. As can be seen in Sec. II B, the logarithmic volume-dependence is quite complex. Therefore, to verify the results of our analytic calculation, we examine a simpler model, namely the  $O(4)$  pure scalar theory and confront the scaling formulae with numerical data from lattice simulations. As shown in Sec. III, it is observed that our formulae fit the numerical data well.

This article is organised as the following. In Sec. II we briefly review the FSS technique and its application near the mean-field fixed point, and discuss our derivation of the scaling formulae for the Higgs-Yukawa model near the Gaussian fixed point. Section III presents the numerical test by confronting our scaling formulae in a simpler model, namely the  $O(4)$  pure scalar theory, with lattice simulations. Our conclusion is in Sec. IV.

## II. FINITE-SIZE SCALING AND THE RENORMALISATION GROUP

The extraction of anomalous dimensions (critical exponents) is of crucial importance for the study of universality classes in a field theory. For this purpose, the technique of FSS is the most commonly-employed approach. In the current project, our primary task is to establish FSS tools for a class of Higgs-Yukawa models (described in Sec. II A) near the Gaussian fixed point. As explained in the rest of this section, this is achieved by extending the strategy developed for pure scalar field theories in Ref. [73].

### A. The Higgs-Yukawa model

We work with the four-dimensional Euclidean Higgs-Yukawa theory that contains one Dirac-fermion doublet,

$$\Psi = \begin{pmatrix} t \\ b \end{pmatrix}, \quad (1)$$

and four real scalar fields,  $\phi_{0,1,2,3}$ , which can be represented in the quaternion form,

$$\Phi = \frac{1}{2} \sum_{\alpha=0}^3 \theta_{\alpha} \phi_{\alpha}, \quad \text{where } \theta_0 = \mathbb{I}_{2 \times 2}, \text{ and } \theta_j = i\sigma_j \ (j = 1, 2, 3), \quad (2)$$

with  $\sigma_j$  being the Pauli matrices. The Lagrangian of this model in Euclidean space in the continuum is

$$\begin{aligned} \mathcal{L}_{\text{HY}} = & \text{Tr} (\partial_{\mu} \Phi^{\dagger} \partial_{\mu} \Phi) + M^2 \text{Tr} (\Phi^{\dagger} \Phi) + \lambda [\text{Tr} (\Phi^{\dagger} \Phi)]^2 \\ & + \bar{\Psi} \not{\partial} \Psi + 2y (\bar{\Psi}_{\text{L}} \Phi \Psi_{\text{R}} + \bar{\Psi}_{\text{R}} \Phi^{\dagger} \Psi_{\text{L}}), \end{aligned} \quad (3)$$

where  $M$  is related to the Higgs-boson mass in the broken phase of the model,  $\lambda$  is the quartic self-coupling of the scalar fields, and  $y$  is the Yukawa coupling. The pure scalar sector of the above model contains the usual  $O(4)$  symmetry. Notice that we are setting the “top” and “bottom” Yukawa couplings to be degenerate. Because of this degeneracy, the operators involving fermions are symmetric under the transformation

$$\Psi_{\text{L}} \longrightarrow U_{\text{L}} \Psi_{\text{L}}, \quad \Psi_{\text{R}} \longrightarrow U_{\text{R}} \Psi_{\text{R}}, \quad \Phi \longrightarrow U_{\text{L}} \Phi U_{\text{R}}^{\dagger}, \quad (4)$$

where  $U_L$  and  $U_R$  are elements of the left- and right-handed  $SU(2)$  groups [ $SU(2)_L$  and  $SU(2)_R$ ], respectively. Since  $SU(2)_L \times SU(2)_R$  covers the  $O(4)$  group, the presence of the Yukawa interactions does not explicitly break the  $O(4)$  symmetry in the scalar sector. In addition to the above symmetries, the Lagrangian in Eq. (3) is invariant under

$$\Psi \longrightarrow \gamma_5 \Psi, \quad \Phi \longrightarrow -\Phi. \quad (5)$$

This ‘‘generalised- $Z_2$ ’’ symmetry will play an important role in deriving the scaling formulae, as explained in the next subsection.

Finally, for convenience, we also define

$$Y = y^2, \quad (6)$$

which exhibits the same classical scaling behaviour as the quartic coupling,  $\lambda$ , in arbitrary space-time dimension.

### B. Derivation of finite-size scaling formulae near the Gaussian fixed point

To investigate universality classes of a theory, it is crucial to understand the renormalisation group (RG) running behaviour of its couplings in the vicinity of critical points. In the study of critical phenomena, such scaling behaviour reveals the character of the associated fixed point. For four-dimensional quantum field theories, a special feature of the Gaussian fixed point is the presence of a double zero in the beta function. This feature results in logarithmic scaling behaviour [2]. In this subsection, we will demonstrate that one can derive mean-field FSS formulae for Higgs-Yukawa model, and the leading logarithms can be obtained by employing one-loop perturbation theory. These logarithms then result in corrections to the mean-field scaling laws.

In our calculations, we analyse the theory in Eq. (3) on an anisotropic box with the four-volume being  $L^3 \times L_t$ , where  $L_t$  is the Euclidean temporal extent. We define the anisotropy in lattice size,

$$s \equiv \frac{L_t}{L}, \quad (7)$$

which is kept constant in our calculation.

We first briefly review the generic argument for FSS, proceeding with the theory described by the Lagrangian in Eq. (3). For this purpose, we investigate a bare matrix element,  $\mathcal{M}_b[M_b^2, \lambda_b, Y_b; a, L]$  of classical (mass) dimension  $D_{\mathcal{M}}$ , where all the external momenta are vanishing. This matrix element depends on the couplings,  $M_b^2$ ,  $\lambda_b$  and  $Y_b$ , which are the bare counterparts of the quadratic, quartic and the Yukawa couplings in Eqs. (3) and (6). We envisage that  $\mathcal{M}_b$  is computed using lattice regularisation. Therefore it is also a function of the lattice spacing,  $a$ , and size,  $L$ . One obtains the corresponding renormalised matrix element in a scheme *via*

$$\mathcal{M}[M^2(l), \lambda(l), Y(l); l, L] = Z_{\mathcal{M}}(l/a) \times \mathcal{M}_b[M_b^2, \lambda_b, Y_b; a, L], \quad (8)$$

where  $l$  is the renormalisation (length-)scale, and the matching coefficient,  $Z_{\mathcal{M}}$ , can usually be determined either numerically or analytically. For convenience, in the discussion below we rescale all dimensionfull quantities by appropriate powers of a common scale, and denote their corresponding, rescaled, dimensionless counterparts with a caret on top. Natural candidates for this common scale can be the lattice spacing,  $a$ , and the renormalisation scale,  $l$ , in Eq. (8).

To observe the FSS behaviour of  $\hat{\mathcal{M}}_b$ , one first performs the RG running from the renormalisation scale  $l$  to  $L$  for  $\hat{\mathcal{M}}$  in Eq. (8). This leads to

$$\begin{aligned} Z_{\mathcal{M}}(\hat{l}/\hat{a}) \times \hat{\mathcal{M}}_b[\hat{M}_b^2, \lambda_b, Y_b; \hat{a}, \hat{L}] &= \hat{\mathcal{M}}[\hat{M}^2(l), \lambda(l), Y(l); \hat{l}, \hat{L}] \\ &= \zeta_{\mathcal{M}}(\hat{l}, \hat{L}) \hat{L}^{-D_{\mathcal{M}}} \hat{\mathcal{M}}[\hat{M}^2(L) \hat{L}^2, \lambda(L), Y(L); 1, 1], \end{aligned} \quad (9)$$

where

$$\zeta_{\mathcal{M}}(\hat{l}, \hat{L}) = \exp \left( \int_{\hat{l}}^{\hat{L}} \gamma_{\mathcal{M}}(\rho) d \log \rho \right), \quad (10)$$

with  $\gamma_{\mathcal{M}}$  being the anomalous dimension of  $\mathcal{M}$ . Assume that there exists a strongly-coupled fixed point in the theory. When the model is near the critical surface of this fixed point at the length scale  $L$ , the renormalised dimensionless couplings,  $\lambda(L)$  and  $Y(L)$ , as well as  $\gamma_{\mathcal{M}}$  approach constants. This results in the scaling formula

$$Z_{\mathcal{M}}(\hat{l}/\hat{a}) \times \hat{\mathcal{M}}_b[\hat{M}_b^2, \lambda_b, Y_b; \hat{a}, \hat{L}] \times \hat{L}^{D_{\mathcal{M}} - \gamma_{\mathcal{M}}} = f_{\mathcal{M}}[\hat{M}^2(L)\hat{L}^2], \quad (11)$$

where

$$\hat{M}^2(L) = \hat{M}^2(l) \left( \frac{L}{l} \right)^{-2+1/\nu_{\mathcal{M}}}, \quad (12)$$

with  $\nu_{\mathcal{M}}$  being the anomalous dimension of this quadratic coupling. The above equation states that in the critical regime, the function,  $f_{\mathcal{M}}$ , depends on only one parameter for all values of  $\hat{L}$ . This is the usual FSS behaviour. Generically, it is not possible to derive the explicit functional form of  $f_{\mathcal{M}}$  for strongly-coupled fixed points. Nevertheless, in this case numerical studies for the scaling properties in Eq. (11) can proceed with the use of the curve-collapse method [74].

It was pointed out by Brezin [72] that care has to be taken when applying the above simple argument for critical points associated with Gaussian fixed points. As discussed in Ref. [73], the incorporation of logarithmic corrections is crucial for deriving mean-field FSS laws in four space-time dimensions. The authors of Ref. [73] developed the detailed techniques for investigating scaling behaviour for pure scalar field theories. In the current work, we extend their results for the first time to the case of the Higgs-Yukawa model of Eq. (3). Below we also demonstrate that near the Gaussian fixed point, explicit scaling functions [ $f_{\mathcal{M}}$  in Eq. (11)] can be obtained at the accuracy of leading logarithms.

Consider the Euclidean partition function of the model in Eq. (3)

$$Z_{\text{HY}} = \int \mathcal{D}\Phi \mathcal{D}\bar{\Psi} \mathcal{D}\Psi \exp \left\{ -S_{\text{HY}}[\Phi, \bar{\Psi}, \Psi] \right\}, \quad (13)$$

where

$$S_{\text{HY}} = \int d^4x \mathcal{L}_{\text{HY}}, \quad (14)$$

with  $\Psi$  and  $\Phi$  defined in Eqs. (1) and (2). To proceed, we first integrate out the fermion fields. This results in

$$Z_{\text{HY}} = \int \mathcal{D}\Phi \exp \left\{ -\tilde{S}_{\text{eff}}[\Phi] \right\}, \quad (15)$$

and  $\tilde{S}_{\text{eff}}$  includes the effects from the fermion determinant. It is straightforward, with an explicit calculation, to show that

$$\tilde{S}_{\text{eff}}[\Phi] = Z_{\Phi} \text{Tr} (\partial_{\mu} \Phi^{\dagger} \partial_{\mu} \Phi) + \tilde{V}_{\text{eff}}[\Phi], \quad (16)$$

where

$$\tilde{V}_{\text{eff}}[\Phi] = \sum_{n=1}^{\infty} g_{2n} [\text{Tr} (\Phi^{\dagger} \Phi)]^n, \quad (17)$$

with  $Z_{\Phi}$  and  $g_n$  being functions of  $M^2$ ,  $\lambda$  and  $Y$ . The fact that  $\tilde{V}_{\text{eff}}$  contains only polynomials of  $[\text{Tr} (\Phi^{\dagger} \Phi)]$  is a consequence of the symmetries described in Eqs. (4) and (5). For the current work, we are interested in investigating this theory near the critical surface of the Gaussian fixed point, where the scaling behaviour only receives logarithmic corrections. In this case, the operators with dimension larger than four can be neglected in  $\tilde{V}_{\text{eff}}$ . That is, this potential can be well approximated by

$$\tilde{V}_{\text{eff}}[\Phi] \approx g_2 \text{Tr} (\Phi^{\dagger} \Phi) + g_4 [\text{Tr} (\Phi^{\dagger} \Phi)]^2. \quad (18)$$

Our goal is to study FSS behaviour of correlators involving only the zero modes of the scalar fields in this theory. We denote these modes by  $\varphi_{\alpha}$  ( $\alpha = 0, 1, 2, 3$ ). They are defined through

$$\varphi_{\alpha} = \frac{1}{V} \int_V d^4x \phi_{\alpha}. \quad (19)$$

Furthermore, we can perform the decomposition

$$\phi_\alpha = \varphi_\alpha + \chi_\alpha, \quad (20)$$

with

$$\int d^4x \chi_a = 0. \quad (21)$$

That is,  $\chi_\alpha$  are the fluctuations around the zero modes. Near the Gaussian fixed point, these fluctuations can be treated perturbatively. In this project, we work with one-loop precision in deriving the FSS formulae. It is straightforward to show that to this order, the contributions to the partition function,  $Z_{\text{HY}}$ , from terms that are quadratic and non-quadratic in  $\chi_a$  are completely factorised. Together with Eqs. (15), (16) and (18), this factorisation allows us to obtain the partition function at one-loop,

$$Z_{\text{HY}}^{1\text{-loop}} = \int_{-\infty}^{\infty} d^4\varphi_\alpha \mathcal{R}_\chi \exp(-S_{\text{eff}}[\varphi_\alpha]) = \mathcal{R}_\chi \Omega_3 \int_0^\infty d\varphi \varphi^3 \exp(-S_{\text{eff}}[\varphi]), \quad (22)$$

where  $\mathcal{R}_\chi$  is the non-quadratic contribution of  $\chi_a$ ,  $S_{\text{eff}}$  is the effective action resulting from integrating out fermion fields and the bosonic degrees of freedom that are quadratic in  $\chi_a$ , the symbol  $\Omega_3$  stands for the four-dimensional solid angle, and  $\varphi$  is defined as

$$\varphi \equiv \sqrt{\sum_{\alpha=0}^3 \varphi_\alpha^2}. \quad (23)$$

In deriving Eq. (22), we use the factorisation of  $\mathcal{R}_\chi$  and the quadratic terms in  $\chi_a$  at one-loop order. This allows us to treat  $\mathcal{R}_\chi$  as an overall normalisation constant, since we are only interested in obtaining scaling formulae for moments of  $\varphi$  at the one-loop precision level. In the rest of this article,  $\mathcal{R}_\chi$  is set to be unity. On the other hand, the path integral over the fermionic degrees of freedom, and the quadratic contributions from  $\chi_a$  result in effects of renormalising the coupling constants in  $S_{\text{eff}}$ . Near the critical surface of the Gaussian fixed point, effects of this one-loop renormalisation can be studied perturbatively with a saddle-point expansion around the zero mode [73]. It is straightforward to demonstrate that this leads to

$$\exp(-S_{\text{eff}}[\varphi]) = \exp(-sL^4 M^2(r)\varphi^2 - sL^4 \lambda(r)\varphi^4), \quad (24)$$

where  $M^2(r)$  and  $\lambda(r)$  are the one-loop renormalised couplings, with  $r$  being the renormalisation (length-)scale.

To proceed with the discussion of the FSS behaviour as governed by the Gaussian fixed point, we first perform the change of variable,

$$\varphi = [sL^4 \lambda(r)]^{-1/4} \check{\varphi}. \quad (25)$$

This enables us to express the partition function in terms of renormalised quantities as [73],

$$Z_{\text{HY}}^{1\text{-loop}} = \Omega_3 [sL^4 \lambda(r)]^{-1} \int_0^\infty d\check{\varphi} \check{\varphi}^3 \exp\left(-\frac{1}{2}z_r \check{\varphi}^2 - \check{\varphi}^4\right), \quad (26)$$

where

$$z_r = \sqrt{s} \hat{L}^2 \hat{M}^2(r) \lambda(r)^{-1/2}. \quad (27)$$

Notice that the dimensionless zero-mode variable,  $\check{\varphi}$ , is obtained by rescaling  $\varphi$  with the lattice size. In the limit where  $L$  is large compared with all the other scales in the theory, this also justifies the approximation of the effective potential,  $\check{V}_{\text{eff}}$ , in Eq. (18).

In order to derive the FSS behaviour of the theory near the Gaussian fixed point, we resort to the general renormalisation-group consideration summarised in Eqs. (9) and (11). Our aim is to investigate the scaling laws for moments of the zero-mode variable,  $\varphi$ , which is also renormalisation-scale dependent. The first step is to identify the above renormalisation scale,  $r$ , as the lattice size,  $L$ . This results in

$$Z_{\text{HY}}^{1\text{-loop}} = \Omega_3 [sL^4 \lambda(L)]^{-1} \check{\varphi}_3(z), \quad \text{and} \quad \langle \varphi^k(L) \rangle = [sL^4 \lambda(L)]^{-k/4} \left[ \frac{\check{\varphi}_{k+3}(z)}{\check{\varphi}_3(z)} \right], \quad (28)$$

with

$$z \equiv z_{\hat{r}}|_{r=L} = \sqrt{s} \hat{L}^2 \hat{M}^2(L) \lambda(L)^{-1/2}, \quad (29)$$

and

$$\bar{\varphi}_n(z) \equiv \int_0^\infty d\tilde{\varphi} \tilde{\varphi}^n \exp\left(-\frac{1}{2}z\tilde{\varphi}^2 - \tilde{\varphi}^4\right). \quad (30)$$

Equations (28) and (29) also demonstrate the failure of the naive FSS argument for the Gaussian fixed point, at which the quartic coupling vanishes. One important step for practical implementation of the strategy in Eqs. (9) and (11) is the matching of the bare lattice quantities to a renormalisation scheme at a length scale  $l$ , followed by the renormalisation-group running to  $L$ . For the  $k$ -th moment of  $\varphi$  in Eq. (28), this means ( $\delta_\varphi$  is the anomalous dimension for  $\varphi$ ),

$$\begin{aligned} \bar{v}_k &\equiv [sL^4 \lambda(L)]^{k/4} \langle \varphi^k(L) \rangle = [s\hat{L}^4 \lambda(L)]^{k/4} \langle \hat{\varphi}^k(L) \rangle \\ &= [s\hat{L}^4 \lambda(L)]^{k/4} \exp\left(k \int_l^{\hat{L}} \delta_\varphi(\rho) d \log \rho\right) \langle \hat{\varphi}^k(l) \rangle \end{aligned} \quad (31)$$

is a function with only one argument,  $z$ . That is, once a matching scale,  $l$  is chosen, and the running is performed, then  $\bar{v}_k$  extracted at different lattice sizes will fall on a universal curve when plotted against  $z$ .

Before presenting further discussion for the details of the renormalisation-group running and the logarithmic volume corrections in  $z$  and  $\varphi$ , we find that the integrals in Eq. (30) can be performed analytically, and the results are

$$\begin{aligned} \bar{\varphi}_0 &= \frac{\pi}{8} \exp\left(\frac{z^2}{32}\right) \sqrt{|z|} \left[ I_{-1/4}\left(\frac{z^2}{32}\right) - \text{Sgn}(z) I_{1/4}\left(\frac{z^2}{32}\right) \right], \\ \bar{\varphi}_1 &= \frac{\sqrt{\pi}}{8} \exp\left(\frac{z^2}{16}\right) \left[ 1 - \text{Sgn}(z) \text{Erf}\left(\frac{|z|}{4}\right) \right], \\ \bar{\varphi}_{n+2} &= -2 \frac{d}{dz} \bar{\varphi}_n, \end{aligned} \quad (32)$$

where  $I_\nu$  is the modified Bessel function of the first kind. In other words, we have discovered that, unlike the generic case for strongly-coupled fixed points, the FSS laws for the Gaussian fixed point can be derived explicitly<sup>1</sup>. To our knowledge, this work is the first derivation of the scaling behaviour encoded in Eqs. (31) and (32), although similar formulae for describing the O(4) pure-scalar theory in the large-volume limit were presented in Ref. [8].

With the results in Eq. (32), in principle one can obtain FSS behaviour for any moment of  $\varphi$ . To use these formulae for investigating the fixed-point structure of the theory through lattice calculations, it is necessary to perform RG running between the matching scale and the lattice size [Eqs. (9) and (11)]. This can be achieved using one-loop perturbation theory, given that the FSS study is carried out in the vicinity of the critical surface associated with the Gaussian fixed point<sup>2</sup>. The use of perturbation theory introduces logarithmic corrections, as well as unknown parameters, to these scaling formulae. To see explicitly how this is implemented, let us begin with the structure of the one-loop renormalisation group equations for the theory in Eq. (3),

$$\begin{aligned} -\rho \frac{d}{d\rho} Y(\rho) &= \beta_{YY^2} Y(\rho)^2, \\ -\rho \frac{d}{d\rho} \lambda(\rho) &= \beta_{\lambda\lambda^2} \lambda(\rho)^2 + \beta_{\lambda\lambda Y} \lambda(\rho) Y(\rho) + \beta_{\lambda Y^2} Y(\rho)^2, \\ -\rho \frac{d}{d\rho} M^2(\rho) &= 2 [\gamma_Y Y(\rho) + \gamma_\lambda \lambda(\rho)] M^2(\rho), \\ -\rho \frac{d}{d\rho} \varphi(\rho) &= 2\delta_Y Y(\rho) \varphi(\rho), \end{aligned} \quad (33)$$

<sup>1</sup> One essential ingredient for making this statement is the truncation of  $\tilde{V}_{\text{eff}}$  in Eq. (18). This truncation may not be applicable for strongly-coupled fixed points, because of the possibility for generating large anomalous dimensions which can qualitatively alter the scaling behaviour of operators.

<sup>2</sup> Notice that Eq. (22) is valid also only at one-loop.

where the anomalous dimensions,  $\beta$ 's,  $\gamma$ 's and  $\delta_Y$  are independent of renormalisation scheme at this order. We find that their values are

$$\begin{aligned}\beta_{YY^2} &= \frac{1}{\pi^2}, \quad \beta_{\lambda\lambda^2} = \frac{6}{\pi^2}, \quad \beta_{\lambda\lambda Y} = \frac{1}{\pi^2}, \quad \beta_{\lambda Y^2} = -\frac{1}{4\pi^2}, \\ \gamma_\lambda &= \frac{3}{2\pi^2}, \quad \gamma_Y = \frac{1}{4\pi^2}, \quad \delta_Y = -\frac{1}{8\pi^2}.\end{aligned}\tag{34}$$

To complete the discussion of the strategy for deriving FSS formulae, we integrate the above RG equations from the scale  $l$  to  $L$ . This results in the scaling variable,

$$\begin{aligned}z &= \left(\frac{4\beta_{\lambda\lambda^2}}{Y(l)}\right)^{1/2} [Y(l)(\beta_+ - \beta_-)]^{\frac{2\gamma_\lambda}{\beta_{\lambda\lambda^2}}} \hat{L}^2 \hat{M}^2(l) \\ &\times \left[1 + Y(l)\beta_{YY^2} \log\left(\frac{\hat{L}}{\hat{l}}\right)\right]^{\frac{1}{2} - \frac{2\gamma_Y}{\beta_{YY^2}} - \frac{\beta_- \gamma_\lambda}{\beta_{YY^2}\beta_{\lambda\lambda^2}}} \\ &\times \frac{\left\{B_+ - B_- \left[1 + Y(l)\beta_{YY^2} \log\left(\frac{\hat{L}}{\hat{l}}\right)\right]^{\frac{\beta_+ - \beta_-}{2\beta_{YY^2}}}\right\}^{\frac{1}{2} - \frac{2\gamma_\lambda}{\beta_{\lambda\lambda^2}}}}{\left\{\beta_- B_+ - \beta_+ B_- \left[1 + Y(l)\beta_{YY^2} \log\left(\frac{\hat{L}}{\hat{l}}\right)\right]^{\frac{\beta_+ - \beta_-}{2\beta_{YY^2}}}\right\}^{\frac{1}{2}}},\end{aligned}\tag{35}$$

where

$$\begin{aligned}\beta_\pm &= (\beta_{YY^2} - \beta_{\lambda\lambda Y}) \pm \sqrt{(\beta_{YY^2} - \beta_{\lambda\lambda Y})^2 - 4\beta_{\lambda\lambda^2}\beta_{\lambda Y^2}}, \\ B_\pm &= Y(l)\beta_\pm - 2\lambda(l)\beta_{\lambda\lambda^2}.\end{aligned}\tag{36}$$

In addition, the RG running of  $\varphi$  is also an essential ingredient in deriving these formulae [see Eqs. (28) and (31)], and it leads to

$$\varphi(L) = \left[1 + Y(l)\beta_{YY^2} \log\left(\frac{\hat{L}}{\hat{l}}\right)\right]^{-\frac{2\delta_Y}{\beta_{YY^2}}} \varphi(l).\tag{37}$$

Results presented in this section can be employed to establish triviality of the Higgs-Yukawa model, or to search for alternative scenarios. When performing the study of the fixed-point structure of the theory, one can confront the lattice data obtained near a critical point to Eqs. (31) and (32), with the scaling variable in Eq. (35). Our scaling formulae should fit the data near critical points that are associated with the Gaussian fixed point. The scaling variable contains several unknown parameters,  $\lambda(l)$ ,  $Y(l)$ ,  $M^2(l)$ , as well as another constant that accounts for the additive mass renormalisation<sup>3</sup>. These parameters arise as the integration constants in obtaining the RG running behaviour *via* solving Eq. (33). They can in principle be determined from fitting the lattice data. Since these parameters are also the values of renormalised couplings at the scale where bare lattice results are matched to a particular scheme, they are scheme-dependent. This means that certain choices of renormalisation scheme may help in reducing the number of free parameters in the fit. One such example will be discussed in the next section. Finally, we stress that the extension of our analysis in this section for theories containing more than one fermion doublet can also be investigated, although it is beyond the scope of our current work.

### III. NUMERICAL TEST IN THE O(4) PURE SCALAR MODEL

The scaling formulae presented in Sec. II are intended for the full Higgs-Yukawa model of Eq. (3), for which they were, in fact, derived for the first time. Ideally, the formulae and the FSS analysis strategy ought to be directly tested

---

<sup>3</sup> In principle, the integration constant,  $\varphi(l)$ , in Eq. (37) is not an unknown parameter, because it is obtained by matching the lattice bare variable to its renormalised counterpart. This matching procedure has to be performed, in order to implement the FSS strategy presented here. However, as discussed in the next subsection, in practice there may be unknown parameters associated with it.

for this case. However, this requires a presently prohibitive numerical effort, and is beyond the scope of this work. We therefore decided to perform this test in the simpler, pure scalar O(4) model. As explained in the previous section, one important ingredient in the derivation of the scaling behaviour at one-loop level is the use of Eqs. (31) and (32). This aspect of the procedure is identical in both the Higgs-Yukawa and the scalar O(4) theories. The LL-improved mean-field scaling behaviours of these two models differ only in the detailed logarithmic volume-dependence in the renormalised couplings. Therefore, confronting our formulae in the pure scalar model with lattice simulations is at least directly testing the validity of Eqs. (31) and (32) for obtaining the FSS properties at this order. Furthermore, the scalar O(4) theory can be considered as the Higgs-Yukawa model in the limit of vanishing Yukawa coupling. Since the natural next-stage examination of results presented in Sec. II should be carried out for the Higgs-Yukawa model with small Yukawa coupling, testing the formulae with data from lattice simulations in this simpler scalar theory should lead to non-trivial information regarding the range of parameters and lattice sizes these formulae can be applied. Also on the theoretical side, concentrating on the scalar O(4) model simplifies the scaling formulae which significantly eases the analysis of the numerical data.

### A. The scalar O(4) model and its finite-size scaling behaviour

The scalar O(4) model is described by the pure-scalar part of Eq. (3). Using the convention  $\phi^T = (\phi_0, \phi_1, \phi_2, \phi_3)$ , the action of this model with lattice regularisation can be expressed as,

$$S[\phi] = \sum_{x \in \Gamma} \left\{ \frac{1}{2} a^2 \phi^T(x) \left[ \sum_{\mu=0}^3 (\phi(x + a\hat{\mu}) + \phi(x - a\hat{\mu}) - 2\phi(x)) \right] \right\} + \sum_{x \in \Gamma} \left[ a^2 M_b^2 \phi^T(x) \phi(x) + \lambda_b a^4 (\phi^T(x) \phi(x))^2 \right], \quad (38)$$

where we use  $\Gamma$  to denote the set of lattice sites. To use information existing in the literature and make educated guess for values of  $\hat{M}_b^2$  when searching for critical points in the theory, it can also be convenient to express the above action with the change of variables

$$a^2 M_b^2 = \frac{1 - 2\tilde{\lambda} - 8\kappa}{\kappa}, \quad \lambda_b = \frac{\tilde{\lambda}}{4\kappa^2}. \quad (39)$$

The logarithmic dependence of  $\hat{L}$  for moments of the scalar-field zero mode in the scalar O(4) model can then be obtained by solving the RGEs, Eq. (33) at  $Y(\rho) = 0$ , and integrating the renormalisation length scale from  $l$  to  $L$ . Note that the anomalous dimensions in Eq. (33) are universal at the leading-order in perturbation theory, although the values of the renormalised couplings are scheme-dependent. Applying the scaling formulae, the couplings renormalised at  $\hat{l}$  are regarded as free parameters. They can be determined by fitting the FSS behaviour of the considered physical observables. In this work, we investigate the scaling behaviour of three observables. The first is the magnetisation, which is defined as the expectation value of the scalar zero-mode,  $\langle \hat{\varphi} \rangle$ . The second is the magnetic susceptibility,  $\hat{\chi}$ ,

$$\hat{\chi} \equiv \hat{V} (\langle \hat{\varphi}^2 \rangle - \langle \hat{\varphi} \rangle^2), \quad (40)$$

where  $\hat{V}$  is the lattice four-volume. Finally, the third is the dimensionless four-point function,  $\chi^{(4)}$ ,

$$\hat{\chi}^{(4)} = \chi^{(4)} = \hat{V} (3\langle \hat{\varphi}^2 \rangle^2 - \langle \hat{\varphi}^4 \rangle). \quad (41)$$

These three observables can be computed in numerical lattice simulations<sup>4</sup>. Their FSS properties are obtained using Eqs. (28), (29), (30) and (31). Rescaling them with appropriate powers of the lattice size,  $\hat{L}$ , it is straightforward to

---

<sup>4</sup> In this section, quantities with a caret on top are dimensionless in lattice units. For instance,  $\hat{\varphi}$  means  $a\varphi$ . See the discussion below Eq. (8).

demonstrate that

$$\langle \hat{\varphi} \rangle \hat{L} = A(l) [s\lambda(L)]^{-1/4} \frac{\bar{\varphi}_4(z)}{\bar{\varphi}_3(z)}, \quad (42)$$

$$\hat{\chi} \hat{L}^{-2} = A(l)^2 s^{1/2} [\lambda(L)]^{-1/2} \left\{ \frac{\bar{\varphi}_5(z)}{\bar{\varphi}_3(z)} - \left[ \frac{\bar{\varphi}_4(z)}{\bar{\varphi}_3(z)} \right]^2 \right\}, \quad (43)$$

$$\hat{\chi}^{(4)} = A(l)^4 [\lambda(L)]^{-1} \left\{ 3 \left[ \frac{\bar{\varphi}_5(z)}{\bar{\varphi}_3(z)} \right]^2 - \frac{\bar{\varphi}_7(z)}{\bar{\varphi}_3(z)} \right\}, \quad (44)$$

where  $A(l)$  is a free parameter associated with the renormalisation of the scalar field, and will be discussed in more detail at the end of this subsection. The one-loop expression for the quartic coupling renormalised at the length scale  $L$  in this model is

$$\lambda(L) = \frac{\lambda(l)}{1 + \beta_{\lambda\lambda^2} \lambda(l) \log\left(\frac{\hat{L}}{l}\right)}, \quad (45)$$

where  $\beta_{\lambda\lambda^2} = 6/\pi^2$ , as given in Eq. (34). For the O(4) pure-scalar field theory, the LL corrections in  $M^2$  and  $\lambda^{-1/2}$  cancel. This means that at one-loop order the combination  $M^2\lambda^{-1/2}$  is independent of the renormalisation scale, although its value is scheme-dependent. For this reason, the scaling variable,  $z$ , at this order in this theory is

$$z = \sqrt{s} M^2(l) L^2 \lambda^{-1/2}(l) = \sqrt{s} \hat{M}^2(l) \hat{L}^2 \lambda^{-1/2}(l). \quad (46)$$

That is, it does not feature any logarithmic  $L$ -dependence.

The FSS formulae, Eqs. (42), (43) and (44) contain four free parameters,  $A(l)$ ,  $\lambda(l)$ ,  $M(l)$  and an additive renormalisation constant in the relationship between the bare quadratic coupling,  $M_b^2$  in Eq. (38), and  $M^2(l)$ . Given that the scaling functions,  $\bar{\varphi}_{3,4,5,7}(z)$ , are already quite complex, see Eq. (32), it is challenging to determine all four parameters *via* fitting these functions to the lattice data. On the other hand, since these free parameters are related to properties of renormalisation of the theory, one may be able to simplify the numerical analysis procedure by working with a particular scheme. For this purpose, in this project we implement the FSS strategy using the on-shell renormalisation scheme, which is defined by relating a pole mass of the scalar field in the infinite-volume limit, denoted as  $m_P$ , to the renormalised coupling  $M(l)$  at the scale

$$l = \frac{1}{m_P}. \quad (47)$$

This pole mass,  $m_P$ , must be much smaller than the cutoff scale such that the running from  $\hat{m}_P^{-1}$  to  $\hat{L}$  can be well described by leading-order perturbation theory. Also, since  $\hat{m}_P$  will in practice be computed by studying lattice numerical data for the scalar-field propagators, one has to ensure that its infinite-volume extrapolation is under control. The above conditions lead to the requirements that  $m_P L \gtrsim 1$  as well as  $\hat{m}_P \ll 1$ . This hierarchy of scales and the FSS strategy we will employ are depicted in Fig. 1.

In the symmetric phase where all four components of the scalar field are equivalent,  $m_P$  can be extracted by studying the propagator of one of  $\phi_{0,1,2,3}$ , and it is connected to the renormalised  $M$  through the simple relation in the on-shell scheme,

$$m_P^2 = M^2(m_P^{-1}) \quad (\text{symmetric phase}), \quad (48)$$

which is indicated by the effective potential of the theory. In the broken phase,  $m_P$  is identified to be the pole mass of the ‘‘Higgs mode’’ that is the field variable obtained by performing a projection operation,

$$H(x) = \sum_{\alpha=0}^3 \frac{\varphi_\alpha}{\varphi} \phi_\alpha(x), \quad \forall x \in \Gamma, \quad (49)$$

where  $\varphi_\alpha$  and  $\varphi$  are defined in Eqs. (19) and (23), respectively. This Higgs field is massive in this phase. One can also construct the three ‘‘Goldstone modes’’ that are perpendicular to  $H(x)$  in the internal O(4) space. These Goldstone

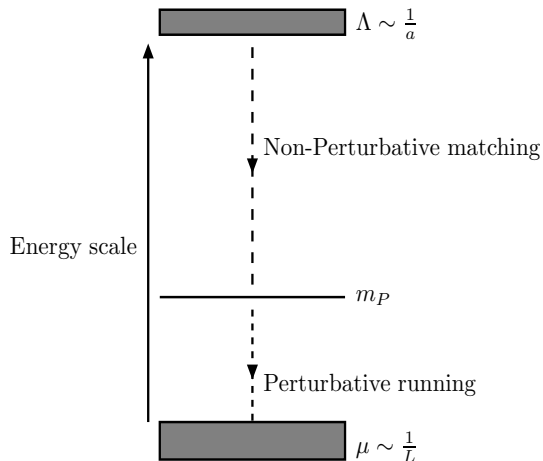


FIG. 1: The scales involved in our FSS strategy with the on-shell renormalisation scheme. Starting from the lattice theory at scale  $\Lambda \propto 1/a$ , we non-perturbatively match bare quantities to the on-shell renormalisation scheme at  $m_P$ , from where we perform a leading-order perturbative running to the energy scale  $\mu \sim 1/L$ .

modes are denoted as  $G(x)$  in this work, and they should be massless. It is straightforward to show that in the broken phase, the implementation of the on-shell scheme results in the condition

$$m_P^2 = -2M^2(m_P^{-1}) \quad (\text{broken phase}). \quad (50)$$

From the above discussion, it is obvious that in the numerical analysis for the scaling test, use of the on-shell renormalisation scheme reduces the number of free parameters from four to two. Since the renormalised mass can be obtained non-perturbatively from studying the lattice data for the scalar-field propagators, one only needs to determine  $A(m_P^{-1})$  and  $\lambda(m_P^{-1})$  from the fits to Eqs. (42), (43) and (44). One aspect in the non-trivial verification of our FSS formulae is the demonstration that employing three different quantities ( $\langle\hat{\varphi}\rangle$ ,  $\hat{\chi}$  and  $\hat{\chi}^{(4)}$ ) to extract  $A(m_P^{-1})$  and  $\lambda(m_P^{-1})$  leads to compatible results.

We close the discussion of the FSS analysis strategy for the O(4) scalar model by elaborating on the introduction of the parameter  $A(l) = A(m_P^{-1})$  in Eqs. (42), (43) and (44). From Eq. (31), it can be seen that there is no integration constant for the running of the moments of the renormalised scalar-field zero mode, if the zero mode is matched from the lattice-regularised theory to the chosen renormalisation scheme, the latter being the on-shell scheme in this work. In general this matching has to be carried out non-perturbatively, since couplings at high-energy scale can be strong in this theory. Very frequently, it is much more convenient to first match the field variable to an “intermediate renormalisation scheme”, *e.g.*, a momentum-subtraction (MOM) scheme. The parameter  $A(m_P^{-1})$  is incorporated in the scaling formulae to account for the connection between the intermediate and the on-shell schemes.

## B. Simulation details

To implement the strategy for testing our FSS formulae as presented in the last subsection, we perform lattice simulations for the O(4) pure scalar field theory described by the action in Eq. (38). In order to realise the hierarchy of scales,

$$a \ll m_P^{-1} \lesssim L, \quad (51)$$

lattices with large size are necessary. For this purpose, we carry out calculations with the spatial volume  $L^3$  at

$$\hat{L} = L/a = 36, 40, 44, 48, 56, \quad (52)$$

and the temporal extent

$$\hat{L}_t = s\hat{L}, \quad s = 2. \quad (53)$$

Furthermore, since our goal is to test the scaling properties governed by the Gaussian fixed point, we choose to proceed with a weak bare quartic coupling,

$$\lambda_b = 0.15, \quad (54)$$

and then simulate at various values of the bare quadratic coupling,  $\hat{M}_b^2$ , to perform a scan and search for phase transitions. Through the initial study of the magnetisation and the susceptibility, we then identify six choices of  $\hat{M}_b^2$  that are close to the critical point. They are

- $\hat{M}_b^2 = -0.54141, -0.54189$  and  $-0.54236$ , corresponding to  $\kappa = 0.131300, 0.131308$  and  $0.131316$ . These points are in the symmetric phase.
- $\hat{M}_b^2 = -0.54334, -0.54349$  and  $-0.54378$ , corresponding to  $\kappa = 0.1313325, 0.131335$  and  $0.131340$ . These points are in the broken phase.

Simulations at other  $\kappa$  values have also been executed. However, these other data points are too far away from the critical point, which makes it impractical to include them in the scaling test.

Since we are carrying out lattice computations near a critical point in the theory, it is necessary to employ an efficient algorithm that can reduce the effects of critical slowing down. For this, we implement a method that combines the Metropolis and the cluster [75] updates. A complete sweep in this algorithm consists of one Metropolis step, where all even (odd) lattice sites are updated sequentially, and 32 cluster updates [75], in each of which at least 10% of the lattice sites are included in the clusters. For each choice of  $\hat{M}_b^2$ , one to three Markov chains are created with hot start. In every Markov chain, the first 200 sweeps are discarded for thermalisation purpose. We then proceed to perform measurements on about 20,000 scalar configurations for each set of bare parameters, at the interval of three sweeps.

### C. Analysis and numerical results

The typical autocorrelation time for the data points used in our analysis is about 20 configurations. In view of this, we bin the data with the bin size being 40 configurations. Statistical analysis is carried out by creating 2,500 bootstrap samples for each bare-parameter set.

In our strategy for the FSS test explained in Sec. III A, the pole mass in the infinite-volume limit,  $m_P$ , is an essential ingredient. The pole mass is extracted by studying the relevant scalar-field propagator in momentum space using our numerical data<sup>5</sup>, and then extrapolated to the infinite-volume limit at fixed lattice spacing, *i.e.*, at fixed value of  $\kappa$ . This extrapolation is performed using an ansatz inspired by the results in Ref. [76],

$$\hat{m}_P^{(\hat{L})} = \hat{m}_P^{(L=\infty)} + \frac{\mathcal{A}}{\hat{L}^2}, \quad (55)$$

where  $\hat{m}_P^{(\hat{L})}$  denotes the pole mass measured from our lattice data in finite volume, while  $\hat{m}_P^{(L=\infty)}$  and  $\mathcal{A}$  are fit parameters, with  $\hat{m}_P^{(L=\infty)}$  being the infinite-volume result,  $\hat{m}_P$ . We have also used the same ansatz to investigate the mass of the Goldstone bosons, and find that it is always compatible with zero in the infinite-volume limit. Figure 2 shows examples of this extrapolation at two values of the bare coupling  $\hat{M}_b^2$ . Results of the pole mass measured on all lattice volumes and extrapolated to the  $\hat{L} \rightarrow \infty$  limit are summarised in Table I and Fig. 3.

When examining the scalar-field propagators, we observe that the residue for all the propagators computed from the lattice data is consistent with one. This means that within our numerical precision, the field variables are already naturally “matched” to a MOM scheme. As discussed at the end of Sec. III A, the connection between this MOM scheme and the on-shell renormalisation scheme can be accounted for by introducing a fit parameter [ $A(m_P^{-1})$  in Eqs. (42), (43) and (44)] in the analysis strategy.

Once the infinite-volume pole mass in lattice units,  $\hat{m}_P$ , is determined for each choice of  $\hat{M}_b^2$ , it can be used to obtain the corresponding renormalised quadratic coupling,  $\hat{M}^2(m_P^{-1})$ , through Eqs. (48) and (50). This quadratic coupling is

---

<sup>5</sup> In the symmetric phase, we average over the modes of  $\phi_{0,1,2,3}$ .

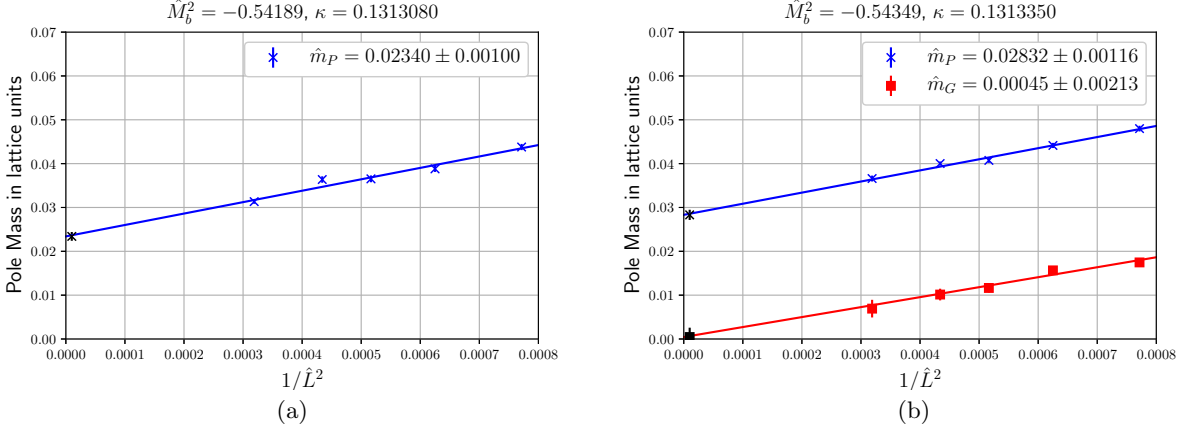


FIG. 2: Examples of the infinite-volume extrapolation for the pole mass in the symmetric (a) and the broken (b) phases using the ansatz of Eq. (55). Results for the Goldstone-boson mass, computed from the average for the propagators of the three Goldstone modes, in the broken phase are also shown in (b).

	Symmetric phase			Broken phase		
$\hat{M}_b^2$	-0.54141	-0.54189	-0.54236	-0.54334	-0.54349	-0.54378
$\kappa$	0.131300	0.131308	0.131316	0.1313325	0.131335	0.131340
$\hat{L} = 36$	0.04459(59)	0.04378(71)	0.04078(119)	0.04580(83)	0.04800(65)	0.05082(60)
$\hat{L} = 40$	0.04334(62)	0.03882(72)	0.03840(102)	0.04151(59)	0.04415(59)	0.04794(72)
$\hat{L} = 44$	0.04129(45)	0.03652(77)	0.03579(74)	0.03813(75)	0.04076(57)	0.04590(51)
$\hat{L} = 48$	0.03755(55)	0.03638(73)	0.03244(69)	0.03554(62)	0.04002(47)	0.04333(50)
$\hat{L} = 56$	0.03606(44)	0.03134(50)	0.02823(52)	0.03325(52)	0.03658(67)	0.04216(76)
$\hat{L} = \infty$	0.02959(79)	0.02340(100)	0.01890(115)	0.02359(100)	0.02831(116)	0.03464(114)

TABLE I: Results of the pole mass in lattice units,  $\hat{m}_P$ , measured on our lattice, and its extrapolation to the infinite-volume limit.

an important ingredient in constructing the scaling variable,  $z$ , in Eq. (46). Since its value at each lattice spacing can be determined numerically from the above procedure, the remaining fit parameters in the scaling formulae of Eqs. (42), (43) and (44) are  $A(m_P^{-1})$  and  $\lambda(m_P^{-1})$ . From the discussion in Sec. III A, it is clear that this infinite-volume pole mass need not take the same value in the symmetric and the broken phases. For this reason, we distinguish  $A(m_P^{-1})$  and  $\lambda(m_P^{-1})$  in these two phases, and denote them as  $(A_{sy}, \lambda_{sy})$  and  $(A_{br}, \lambda_{br})$ , respectively. That is, in fitting our data for the magnetisation, the susceptibility and the fourth moment of the scalar-field zero mode to Eqs. (42), (43) and (44), there are four unknown parameters ( $A_{sy}, \lambda_{sy}, A_{br}$  and  $\lambda_{br}$ ) to be determined. With the knowledge of these four parameters, the scaling formulae then predict that the “rescaled” quantities,

$$\langle \hat{\varphi} \rangle_{rs} = \langle \hat{\varphi} \rangle \hat{L} \times A(m_P^{-1})^{-1} [s\lambda(L)]^{1/4}, \quad (56)$$

$$\hat{\chi}_{rs} = \hat{\chi} \hat{L}^{-2} \times A(m_P^{-1})^{-2} s^{-1/2} [\lambda(L)]^{1/2}, \quad (57)$$

$$\hat{\chi}_{rs}^{(4)} = \hat{\chi}^{(4)} \times A(m_P^{-1})^{-4} [\lambda(L)], \quad (58)$$

with  $\lambda(L)$  given in Eq. (45) at  $l = 1/m_P$ , exhibit universality. That is, when plotted against the scaling variable,  $z$ , each of them should collapse to a common curve. We stress again that in the above equations,  $[A(m_P^{-1}), \lambda(m_P^{-1})]$  actually means  $(A_{sy}, \lambda_{sy})$  and  $(A_{br}, \lambda_{br})$  in the symmetric and broken phases, respectively.

Results of the individual fits to the FSS formulae, Eqs. (42), (43) and (44), for the magnetisation, the susceptibility and the fourth zero-mode moment, are shown in in Figs. 4(a),(c),(e). Their corresponding rescaled quantities defined in Eqs. (56), (57) and (58) are plotted against the scaling variable in Figs. 4(b),(d),(f). As can be seen, these fits lead to good  $\chi^2$  per degree of freedom (denoted as  $\chi_r^2$  in this work), and scaling behaviour is indeed observed. More importantly, these separate fits for  $\langle \hat{\varphi} \rangle$ ,  $\hat{\chi}$  and  $\hat{\chi}^{(4)}$  result in compatible values of  $A_{sy}, \lambda_{sy}, A_{br}$  and  $\lambda_{br}$ . This demonstrates evidence for the validity of the strategy we designed in Sec. II.

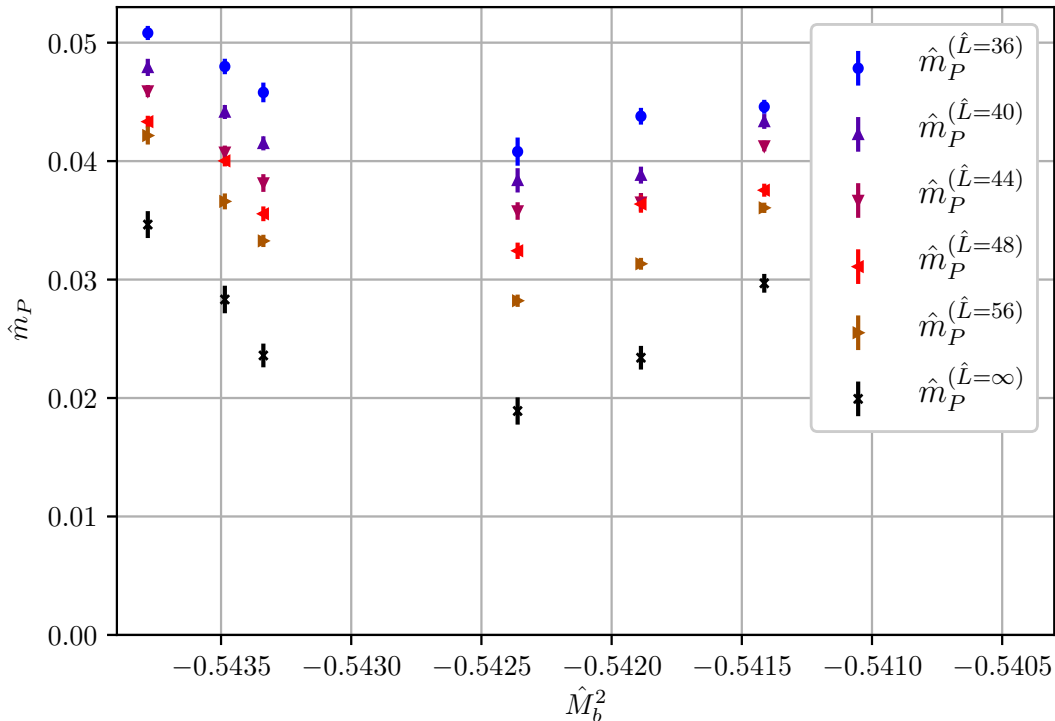


FIG. 3: The infinite volume extrapolations of the pole mass  $m_P$  in lattice units.

To have more stringent test for our scaling formulae, we also perform simultaneous fits to  $\langle\hat{\varphi}\rangle$ ,  $\hat{\chi}$  and  $\hat{\chi}^{(4)}$ . Results of this analysis procedure are displayed in Fig. 5. Compared to the individual fits discussed in the last paragraph, it is more challenging to have good  $\chi_r^2$  ( $\equiv \chi^2/\text{dof}$ ) in this “global fit”, because of a much larger number of data points involved. Nevertheless, we still find reasonable  $\chi_r^2$  in this procedure, and the scaling behaviour is also observed. Furthermore the fit parameters,  $A_{sy}$ ,  $\lambda_{sy}$ ,  $A_{br}$  and  $\lambda_{br}$ , determined using this method are comparable with those extracted from the individual-fit analysis.

Table II lists the parameters,  $A_{sy}$ ,  $\lambda_{sy}$ ,  $A_{br}$  and  $\lambda_{br}$ , together with  $\chi_r^2$ , obtained from the above strategies. Also tabulated are results from simultaneous FSS fits for two observables amongst  $\langle\hat{\varphi}\rangle$ ,  $\hat{\chi}$  and  $\hat{\chi}^{(4)}$ . This table shows that all these fits find an overall agreement on the values of  $A_{sy}$ ,  $\lambda_{sy}$ ,  $A_{br}$  and  $\lambda_{br}$ . In addition, the  $\chi_r^2$  is always acceptable, suggesting that our scaling formulae describe the numerical data in a satisfactory fashion. Finally, we have also tried the scaling tests without logarithms *i.e.*, by setting  $\lambda(\hat{L}) = \lambda(\hat{m}_P^{-1})$  in the scaling formulae, Eqs. (42), (43) and (44). Results from this procedure are in the rows marked as “without Logs” in Table II. These results seem to indicate that our data are still not sensitive to the logarithms. To detect these logarithmic volume-dependence, even larger lattices and an increased accuracy need to be reached. The fact that we are finding it very challenging to identify LL corrections to the mean-field scaling laws is consistent with results from a recent study of the  $Z_2$  scalar field theory presented in Ref. [11], where the authors adopt a slightly different approach from ours. Here we stress that although our data do not allow us to discern the LL contributions in the scaling laws, the test presented in this section is already offering non-trivial information. As discussed in Sec. II B, the use of Eqs. (31) and (32) in obtaining the FSS formulae is justified only for the Gaussian fixed point. This aspect of the derivation is identical for the Higgs-Yukawa and the pure-scalar O(4) models. In other words, the scaling behaviour of  $\langle\hat{\varphi}\rangle$ ,  $\hat{\chi}$  and  $\hat{\chi}_4$  in these two models take the same functional form in Eqs. (42), (43) and (44), with the difference being the explicit logarithmic volume-dependence encoded in  $\lambda$  and  $z$ . In view of this, the fact that our formulae fit the lattice data well is already indicating the validity of employing Eqs. (31) and (32) for the investigation of scaling behaviour governed by the Gaussian fixed point. Furthermore, the pure-scalar O(4) theory can be regarded as the Higgs-Yukawa model in the limit where the

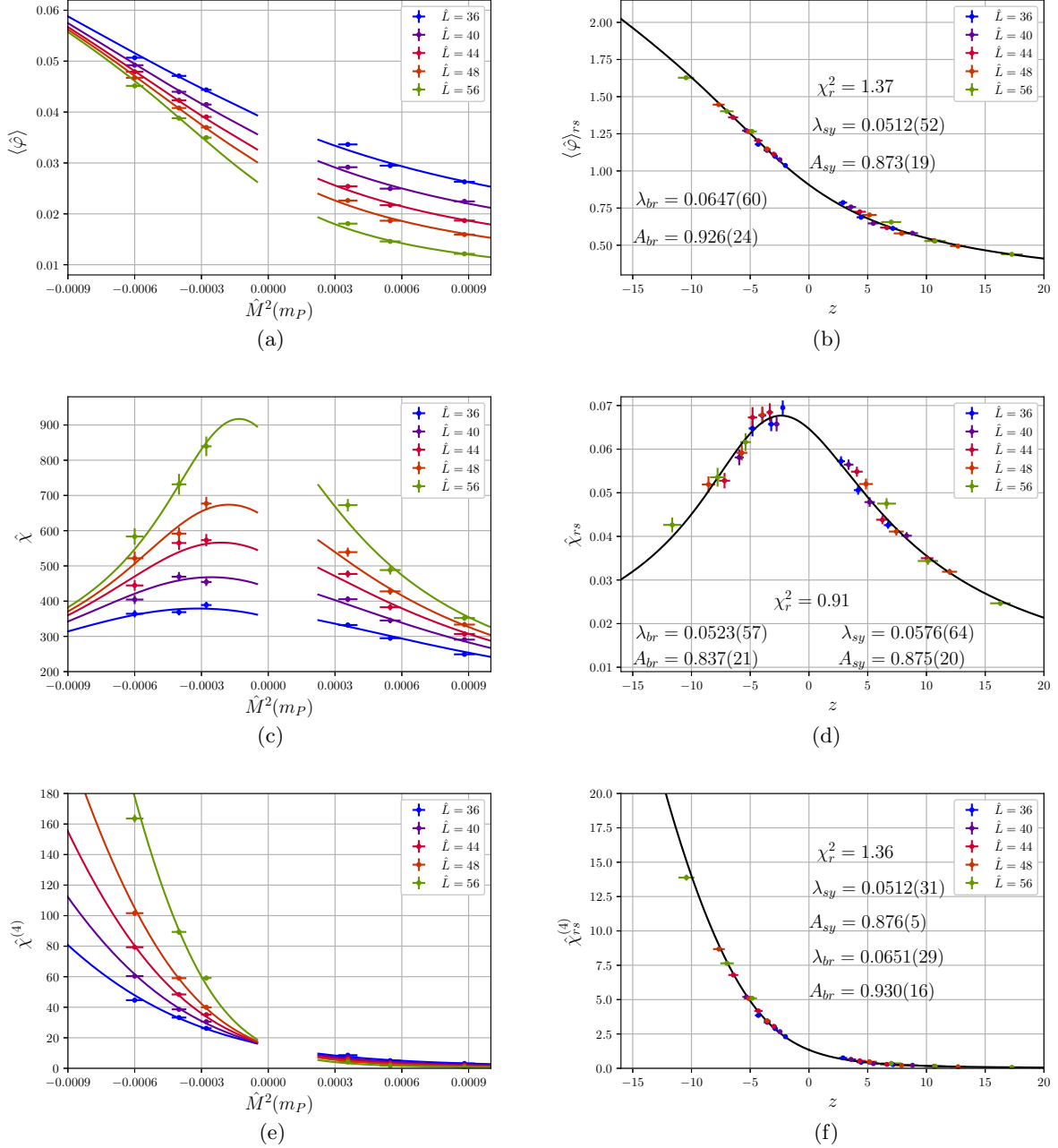


FIG. 4: Results of the scaling tests *via* fitting  $\langle\hat{\varphi}\rangle$ ,  $\hat{\chi}$  and  $\hat{\chi}^{(4)}$  separately to Eqs. (42), (43) and (44) are displayed in (a), (c) and (e). The corresponding rescaled quantities defined in Eqs. (56), (57) and (58) are plotted against the scaling variable in (b), (d) and (f).

Yukawa coupling vanishes. As the first step, this is a meaningful limit to examine our formulae, since the next-stage test of our analytic results should be performed in the Higgs-Yukawa model with small Yukawa coupling. Therefore, this scalar-theory numerical exercise can be taken as a good prototype study for our future investigation of the Higgs-Yukawa model. Since simulations for the Higgs-Yukawa model is very demanding in computing resources, it is especially essential to perform such a prototype study to identify possible range of parameters (*e.g.*, the lattice volumes needed) that would be needed to observe scaling behaviour.

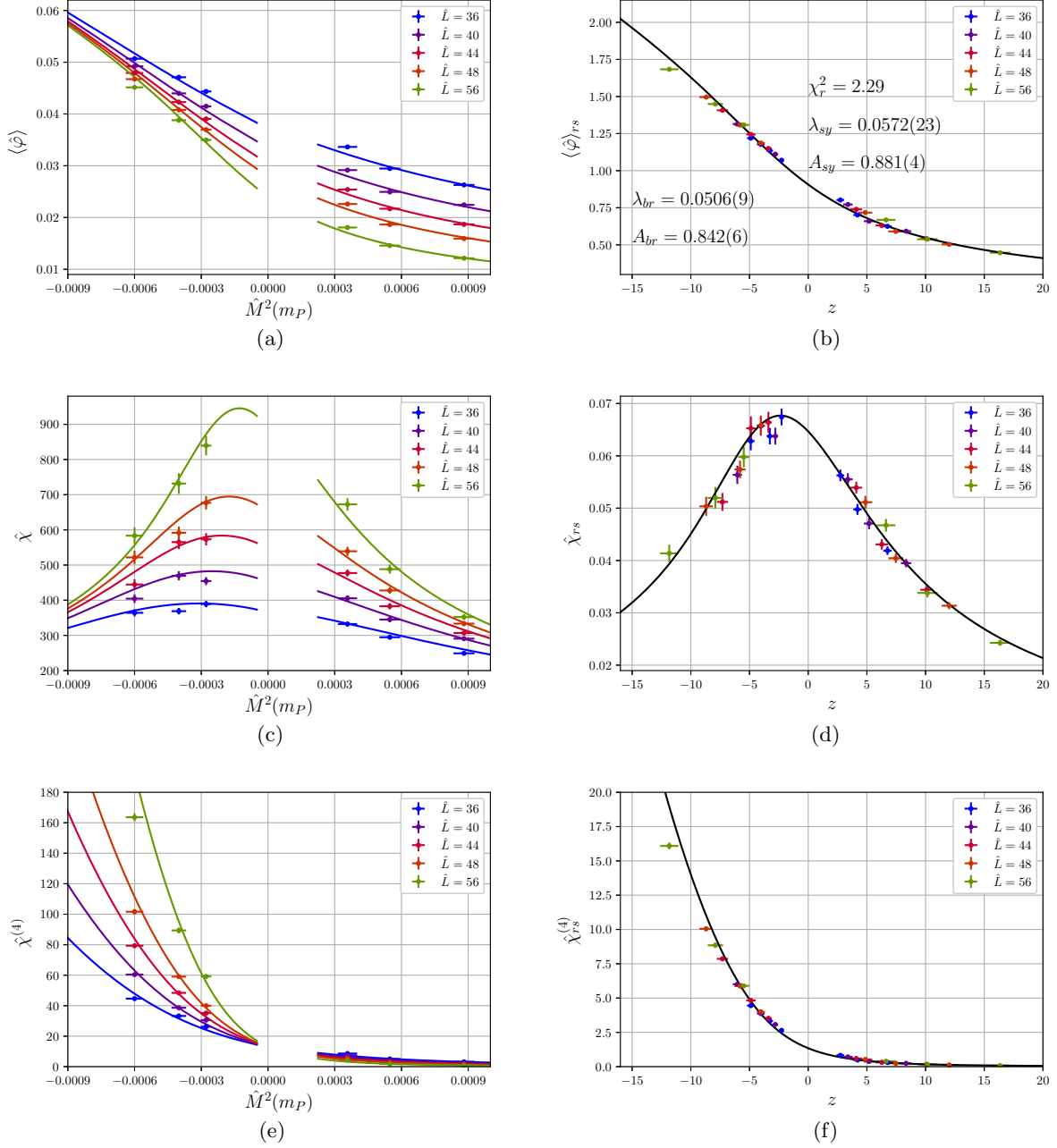


FIG. 5: Result of the scaling test *via* fitting  $\langle \hat{\varphi} \rangle$ ,  $\hat{\chi}$  and  $\hat{\chi}^{(4)}$  simultaneously to Eqs. (42), (43) and (44) are displayed in (a), (c) and (e). The corresponding rescaled quantities defined in Eqs. (56), (57) and (58) are plotted against the scaling variable in (b), (d) and (f).

As discussed earlier in this subsection, our data indicate that within our numerical accuracy, the field variables can be assumed to be already naturally matched to a MOM scheme, leading to the introduction of  $A(m_P^{-1})$  in the scaling formulae to accommodate the matching from this MOM scheme to the on-shell scheme. To examine this assumption, we carry out the fits by allowing  $\kappa$ -dependence (hence lattice-spacing-dependence) in  $A(m_P^{-1})$ . These  $\kappa$ -dependent  $A(m_P^{-1})$  can be interpreted as the matching coefficients between the bare lattice  $\varphi$  and its renormalised counterpart in the on-shell scheme. It is found that this procedure results in values of  $A(m_P^{-1})$  and  $\lambda(m_P^{-1})$  that are well consistent

	$\lambda_{sy}$	$\lambda_{br}$	$A_{sy}$	$A_{br}$	$\chi_r^2$
$\langle\hat{\phi}\rangle$	0.0512(52)	0.0647(60)	0.873(19)	0.926(24)	1.37
without Logs	0.0539(57)	0.0618(54)	0.878(20)	0.910(22)	1.35
$\hat{\chi}$	0.0576(64)	0.0523(57)	0.875(20)	0.837(21)	0.91
without Logs	0.0605(71)	0.0541(62)	0.882(21)	0.843(22)	0.90
$\hat{\chi}^{(4)}$	0.0512(31)	0.0651(29)	0.876(5)	0.930(16)	1.36
without Logs	0.0538(34)	0.0621(26)	0.880(5)	0.914(15)	1.34
$\langle\hat{\phi}\rangle$ and $\hat{\chi}^{(4)}$	0.0513(30)	0.0649(29)	0.875(5)	0.928(16)	1.32
without Logs	0.0539(34)	0.0619(26)	0.880(5)	0.913(15)	1.30
$\langle\hat{\phi}\rangle$ and $\hat{\chi}$	0.0582(22)	0.0494(9)	0.880(4)	0.833(6)	2.08
without Logs	0.0610(24)	0.0502(9)	0.886(9)	0.837(6)	1.84
$\hat{\chi}$ and $\hat{\chi}^{(4)}$	0.0596(22)	0.0490(9)	0.884(4)	0.832(6)	2.24
without Logs	0.0627(25)	0.0499(9)	0.890(4)	0.837(6)	1.98
Global fit	0.0572(23)	0.0506(9)	0.880(4)	0.842(6)	2.29
without Logs	0.0601(25)	0.0514(10)	0.887(4)	0.847(6)	2.01

TABLE II: A summary of all fit parameters from all scaling tests performed: individual, global and combination of two observables.

with those listed in Table II.

We conclude this section by stating the remark that we find the renormalised quartic coupling always to be about a factor of three smaller than the bare one. This shows a strong renormalisation effect in the expected direction, providing further evidence that our strategy is valid.

#### IV. CONCLUSION

In this work, we derive for the first time FSS formulae for the moments of the scalar-field zero mode in a four-dimensional Higgs-Yukawa model. It is found that near the Gaussian fixed point, the scaling laws can be derived for these moments by following the strategy outlined in Ref. [73]. We discuss in detail the incorporation of the leading-logarithmic corrections to these scaling laws *via* solving the one-loop RG equations for the theory. The solution to these equations involves integration constants which appear in the expression of the scalar zero-mode moments, and in the scaling variable. These integration constants can be treated as free parameters that can in principle be extracted by fitting lattice-simulation data with our scaling formulae. Through investigating the quality of such fits, one can determine whether or not particular critical points are associated with the Gaussian fixed point. That is, our formulae can be used to establish the triviality property of the Higgs-Yukawa model at numerical accuracy that can be achieved, or to search for alternative scenarios in the phase structure of the theory.

To examine the scaling laws derived in this project, we confront them with data from numerical simulations in lattice field theory. Since the FSS behaviour of the Higgs-Yukawa model is rather complex, and large-volume simulations of the model are presently very expensive, in the current project we proceed to implement the test in a simpler model, namely the O(4) pure scalar theory. In particular, we study the volume-dependence in three quantities: the magnetisation, the susceptibility and the fourth moment constructed from the zero mode of the scalar field. Compared with the Higgs-Yukawa model, although the functional form of the FSS formulae described by Eqs. (31) and (32) remains the same in this pure scalar theory, the scaling variable simplifies significantly. In addition to performing fits to the above observables separately, we investigate the global fit by determining the free parameters in the scaling behaviour from these three quantities simultaneously. Reasonable fits and compatible results are obtained from both approaches, employing simulations carried out with a weak bare quartic coupling near the critical point at five values of the lattice size in the range  $36 \leq L/a \leq 56$ . This shows that our scaling formulae are indeed valid. On the other hand, we also discover that our data are not sensitive to the effects of the LL corrections to the mean-field scaling laws. However, it is always challenging to concretely discern logarithmic behaviour in scaling tests, and we conclude that numerical calculations at bigger lattice volumes are needed for this aspect of the test, which is beyond the scope of the current work.

The above numerical analysis demonstrates that large lattice sizes can be essential for the scaling test of the Higgs-

Yukawa model. This means that future dedicated efforts and long-term research programmes will be necessary for this task. It is, withal, crucial to have such a test for our understanding of non-perturbative aspects of the SM. Our FSS formulae presented in Sec. II B of this article can eventually be employed to examine the fixed-point structure at large values of the Yukawa coupling [62, 70]. In addition, these formulae could be generalised to more flavours of quarks and possibly to different dimensions as well as the inclusion of gauge fields, making them applicable for similar studies of a broader class of Higgs-Yukawa systems in high-energy and condensed-matter physics [77–81].

### Acknowledgments

The authors thank Philipp Gerhold, Chung-Wen Kao and Attila Nagy for useful discussions. DYJC and CJDL are supported by Taiwanese MoST *via* grant 105-2112-M-002-023-MY3. Numerical calculations have been carried out on the HPC facilities at National Chiao-Tung University and DESY Zeuthen computer centre, as well as on SGI system HLRN-II at HLRN supercomputing service Berlin-Hannover.

- 
- [1] M. Aizenman, Phys.Rev.Lett. **47**, 886 (1981).
- [2] J. Frohlich, Nucl.Phys. **B200**, 281 (1982).
- [3] M. Luscher and P. Weisz, Nucl. Phys. **B290**, 25 (1987).
- [4] M. Luscher and P. Weisz, Nucl. Phys. **B295**, 65 (1988).
- [5] M. Luscher and P. Weisz, Nucl. Phys. **B318**, 705 (1989).
- [6] W. Bernreuther and M. Gockeler, Nucl.Phys. **B295**, 199 (1988).
- [7] R. Kenna and C. Lang, Nucl.Phys. **B393**, 461 (1993).
- [8] M. Gockeler, H. A. Kastrup, T. Neuhaus, and F. Zimmermann, Nucl. Phys. **B404**, 517 (1993), hep-lat/9206025.
- [9] U. Wolff, Phys. Rev. **D79**, 105002 (2009), 0902.3100.
- [10] P. Weisz and U. Wolff, Nucl. Phys. **B846**, 316 (2011), 1012.0404.
- [11] M. Hogervorst and U. Wolff, Nucl. Phys. **B855**, 885 (2012), 1109.6186.
- [12] J. Siefert and U. Wolff, Phys. Lett. **B733**, 11 (2014), 1403.2570.
- [13] R. F. Dashen and H. Neuberger, Phys.Rev.Lett. **50**, 1897 (1983).
- [14] A. Hasenfratz, K. Jansen, C. B. Lang, T. Neuhaus, and H. Yoneyama, Phys.Lett. **B199**, 531 (1987).
- [15] J. Kuti, L. Lin, and Y. Shen, Phys.Rev.Lett. **61**, 678 (1988).
- [16] M. Luscher and P. Weisz, Phys.Lett. **B212**, 472 (1988).
- [17] V. Branchina and E. Messina, Phys.Rev.Lett. **111**, 241801 (2013).
- [18] H. Gies, C. Gneiting, and R. Sondenheimer, Phys.Rev. **D89**, 045012 (2014).
- [19] D. Y.-J. Chu, K. Jansen, B. Knippschild, C.-J. D. Lin, and A. Nagy, Phys.Lett. **B744**, 146 (2015).
- [20] J. Brehmer, A. Freitas, D. López-Val and T. Plehn, Phys. Rev. **D93**, 075014 (2016), 1510.03443.
- [21] A. Biekötter, J. Brehmer, Johann and T. Plehn, Phys. Rev. **D94**, 055032 (2016), 1602.05202.
- [22] D. Y. J. Chu, K. Jansen, B. Knippschild, and C. J. D. Lin, EPJ Web Conf. **175**, 08017 (2018), 1710.09737.
- [23] S. Dawson, in *Proceedings, Theoretical Advanced Study Institute in Elementary Particle Physics : Anticipating the Next Discoveries in Particle Physics (TASI 2016): Boulder, CO, USA, June 6-July 1, 2016* (2017), pp. 1–63, 1712.07232.
- [24] B. Holdom, Phys. Lett. **150B**, 301 (1985).
- [25] K. Yamawaki, M. Bando, and K.-i. Matumoto, Phys. Rev. Lett. **56**, 1335 (1986).
- [26] T. W. Appelquist, D. Karabali, and L. C. R. Wijewardhana, Phys. Rev. Lett. **57**, 957 (1986).
- [27] B. Lucini, arXiv:1503.00371.
- [28] D. Nogradi and A. Patella, Int. J. Mod. Phys. **A31**, 1643003 (2016), 1607.07638.
- [29] B. Svetitsky, EPJ Web Conf. **175**, 01017 (2018), 1708.04840.
- [30] M. Piai, Adv.High Energy Phys. **2010**, 464302 (2010).
- [31] M. Piai, in *Proceedings, KMI-GCOE Workshop on Strong Coupling Gauge Theories in the LHC Perspective (SCGT 12): Nagoya, Japan, December 4-7, 2012* (2014), pp. 185–191.
- [32] D. B. Kaplan, H. Georgi, and S. Dimopoulos, Phys. Lett. **136B**, 187 (1984).
- [33] H. Georgi and D. B. Kaplan, Phys. Lett. **145B**, 216 (1984).
- [34] M. J. Dugan, H. Georgi, and D. B. Kaplan, Nucl. Phys. **B254**, 299 (1985).
- [35] J. Barnard, T. Gherghetta, and T. S. Ray, JHEP **02**, 002 (2014), 1311.6562.
- [36] G. Ferretti and D. Karateev, JHEP **03**, 077 (2014), 1312.5330.
- [37] G. Cacciapaglia and F. Sannino, JHEP **04**, 111 (2014), 1402.0233.
- [38] A. Belyaev, G. Cacciapaglia, H. Cai, G. Ferretti, T. Flacke, A. Parolini, and H. Serodio, JHEP **01**, 094 (2017), [Erratum: JHEP12,088(2017)], 1610.06591.
- [39] T. DeGrand, Y. Liu, E. T. Neil, Y. Shamir, and B. Svetitsky, Phys. Rev. **D91**, 114502 (2015), 1501.05665.
- [40] V. Ayyar, T. DeGrand, M. Golterman, D. C. Hackett, W. I. Jay, E. T. Neil, Y. Shamir, and B. Svetitsky, Phys. Rev. **D97**, 074505 (2018), 1710.00806.
- [41] V. Ayyar, T. DeGrand, D. C. Hackett, W. I. Jay, E. T. Neil, Y. Shamir, and B. Svetitsky, Phys. Rev. **D97**, 114505 (2018), 1801.05809.
- [42] V. Ayyar, T. DeGrand, D. C. Hackett, W. I. Jay, E. T. Neil, Y. Shamir, and B. Svetitsky, Phys. Rev. **D97**, 114502 (2018), 1802.09644.
- [43] E. Bennett, D. K. Hong, J.-W. Lee, C. J. D. Lin, B. Lucini, M. Piai, and D. Vadicchino, JHEP **03**, 185 (2018), 1712.04220.
- [44] J.-W. Lee, Bennett, D. K. Hong, C. J. D. Lin, B. Lucini, M. Piai, and D. Vadicchino, PoS **LATTICE2018**, 192 (2018), 1811.00276.
- [45] P. Hung and C. Xiong, Nucl.Phys. **B847**, 160 (2011).
- [46] E. Molgaard and R. Shrock, Phys.Rev. **D89**, 105007 (2014).
- [47] J. Shigemitsu, Phys.Lett. **B189**, 164 (1987).
- [48] I.-H. Lee and R. E. Shrock, Phys.Rev.Lett. **59**, 14 (1987).
- [49] I.-H. Lee and R. E. Shrock, Nucl.Phys. **B305**, 305 (1988).
- [50] W. Bock, A. De, K. Jansen, J. Jersak, and T. Neuhaus, Phys.Lett. **B231**, 283 (1989).
- [51] A. Hasenfratz, W.-q. Liu, and T. Neuhaus, Phys.Lett. **B236**, 339 (1990).
- [52] I.-H. Lee, J. Shigemitsu, and R. E. Shrock, Nucl.Phys. **B330**, 225 (1990).

- [53] I.-H. Lee, J. Shigemitsu, and R. E. Shrock, Nucl.Phys. **B334**, 265 (1990).
- [54] J. Shigemitsu, Phys.Lett. **B226**, 364 (1989).
- [55] A. Abada and R. Shrock, Phys.Rev. **D43**, 304 (1991).
- [56] W. Bock et al., Nucl.Phys. **B344**, 207 (1990).
- [57] W. Bock, A. K. De, C. Frick, K. Jansen, and T. Trappenberg, Nucl.Phys. **B371**, 683 (1992).
- [58] W. Bock, A. K. De, and J. Smit, Nucl.Phys. **B388**, 243 (1992).
- [59] W. Bock, A. K. De, C. Frick, J. Jersak, and T. Trappenberg, Nucl.Phys. **B378**, 652 (1992).
- [60] A. Hasenfratz, P. Hasenfratz, K. Jansen, J. Kuti, and Y. Shen, Nucl.Phys. **B365**, 79 (1991).
- [61] J. Kuti, in Proceedings of "Electroweak symmetry breaking", Hiroshima 1991.
- [62] A. Hasenfratz, K. Jansen, and Y. Shen, Nucl.Phys. **B394**, 527 (1993).
- [63] L. Maiani, M. Testa, and G. Rossi, Nucl.Phys.Proc.Suppl. **29B+C** (1992).
- [64] Z. Fodor, K. Holland, J. Kuti, D. Nogradi, and C. Schroeder, PoS **LAT2007**, 056 (2007).
- [65] P. Gerhold and K. Jansen, JHEP **0709**, 041 (2007).
- [66] P. Gerhold and K. Jansen, JHEP **0710**, 001 (2007).
- [67] P. Gerhold and K. Jansen, JHEP **0907**, 025 (2009).
- [68] P. Gerhold and K. Jansen, JHEP **1004**, 094 (2010).
- [69] P. Gerhold, K. Jansen, and J. Kallarackal, Phys.Lett. **B710**, 697 (2012).
- [70] J. Bulava et al., Adv.High Energy Phys. **2013**, 875612 (2013).
- [71] M. E. Fisher and M. N. Barber, Phys.Rev.Lett. **28**, 1516 (1972).
- [72] E. Brezin, J.Phys.(France) **43**, 15 (1982).
- [73] E. Brezin and J. Zinn-Justin, Nucl.Phys. **B257**, 867 (1985).
- [74] S. M. Bhattacharjee and F. Seno, Journal of Physics A: Mathematical and General **34**, 6375 (2001), URL <http://stacks.iop.org/0305-4470/34/i=33/a=302>.
- [75] U. Wolff, Phys. Rev. Lett. **62**, 361 (1989).
- [76] P. Hasenfratz and H. Leutwyler, Nucl. Phys. **B343**, 241 (1990).
- [77] M. Shaposhnikov and C. Wetterich, Phys. Lett. **B683**, 196 (2010), 0912.0208.
- [78] H. Gies, S. Rechenberger, M. M. Scherer, and L. Zambelli, Eur. Phys. J. **C73**, 2652 (2013), 1306.6508.
- [79] D. F. Litim and F. Sannino, JHEP **12**, 178 (2014), 1406.2337.
- [80] A. Maas (2017), 1712.04721.
- [81] A. Eichhorn and A. Held, Phys. Rev. **D96**, 086025 (2017), 1705.02342.